Received: January 19, 2023. Revised: February 17, 2023. 546

International Journal of
Intelligent Engineering & Systems

http://www.inass.org/

MobileNetV2 Ensemble Segmentation for Mandibular on Panoramic Radiography

Nur Nafi'iyah[1,3] Chastine Fatichah[1]* Darlis Herumurti[1] Eha Renwi Astuti[2] Ramadhan Hardani Putra[2]

[1]*Department of Informatics, Institut Teknologi Sepuluh Nopember, Surabaya, Indonesia*
[2]*Department of Dentomaxillofacial Radiology, Faculty of Dental Medicine, Universitas Airlangga, Surabaya, Indonesia*
[3]*Department of Informatics, Universitas Islam Lamongan, Lamongan, Indonesia*
* Corresponding author's Email: chastine@if.its.ac.id

Abstract: Mandibular segmentation is an important step in gender identification and age estimation, which aims to segment the mandible from intact and complete panoramic radiograph. One of the main drawbacks of most existing mandibular segmentation methods is that they cannot completely represent the mandible. When conducting several segmentation experiments with several methods, namely U-Net, MobileNetV2, ResNet18, ResNet50, Xception, InceptionResNet V2, MobileNetV2 turned out to be superior. However, if you only use the MobileNetV2 method, the results still need to be clarified on the coronoid and mandibular condyles. Then it is necessary to add an ensemble so that the mandibular segmentation results become more intact and complete. In contrast to the usual MobileNetV2, the mandibular segmentation results are assembled to achieve a complete and intact performance. Finally, this method experimented with 38 panoramic radiographs verified by radiologists. The experimental results show that the proposed MobileNetV2 ensemble for segmentation was superior to the usual MobileNetV2 method with a dice value of 0.9655.

Keywords: Mandibular segmentation, Panoramic radiography, Ensemble segmentation, MobileNetV2.

1. Introduction

Mandibular segmentation aims to segment the mandible from panoramic radiographs widely used in gender identification and age estimation [1]. Accurate segmentation of the mandible is a key step in identifying the forensic team. Mandibular segmentation has previously been performed on CT scan images [2-7], CBCT [8, 9], and panoramic radiographs [10, 11]. However, the mandibular segmentation in the previous research had problems in terms of the mandible did not display the condyle and coronoid completely and clearly. The unclear results of segmentation of the coronoid and condyle mandible are because the panoramic radiographic image has homogeneous intensity values. In addition, it is difficult to distinguish between mandibular objects and teeth or other parts.

To overcome the aforementioned problems, several methods have been proposed for mandibular segmentation, such as symmetric convolution neural network [2], convolutional neural network [3, 6, 8], fuzzy connectivity [4], graph clustering [7], and active contour [10, 11]. The proposed methods for mandibular segmentation are generally divided into traditional methods [4, 7, 10, 11] with an evaluation result of approximately 60% and methods based on the deep neural network [2, 3, 6, 8] with evaluation results of more than 70%.

This research mainly aims to segment the mandible by representing the intact and complete mandible. A method based on the deep neural network was proposed to produce an intact and complete mandible. The evaluation result using the deep neural network method in previous researches was above 70% [2, 3, 6, 8]. Previous researches

used a symmetrically based deep neural network or convolutional neural network (CNN) [2], RCNNSeg [3], adopted the U-Net architecture [6], and SegUnet [8]. Meanwhile, this research adopts the MobileNetV2 architecture, which is ensembled.

Radiographic image that noise and difficulty distinguishing between mandibular objects and teeth can be overcome by enhancing panoramic radiographs with the Ying [12, 13] and DHE [14, 15] methods. Furthermore, the results of enhancing the panoramic radiographic image using the Ying and DHE methods are segmented using the MobileNetV2 method.

The novelty of this research is that ensemble MobileNetV2 was used for mandibular segmentation instead of for classification as usual. Because MobileNetV2 is superior to the U-Net, MobileNetV2, ResNet18, ResNet50, Xception, and InceptionResNet V2 methods when performing mandibular segmentation. However, if you only use the MobileNetV2 method, the results still need to be clarified on the coronoid and mandibular condyles. The original radiographic segmentation results on images that are too dark or too light are not good. The results of enhancing Ying and DHE radiographic segmentation could be better. We propose to combine the three original and enhanced Ying and DHE radiographic segmentation results. Then it is necessary to add an ensemble so that the mandibular segmentation results become more intact and complete. The proposed ensemble segmentation is based on majority voting [16] from the segmentation results of the original panoramic radiography image using the image enhancement Ying and DHE methods. The main contributions in this research are as follows: performing ensemble segmentation to improve intact and complete segmentation results.

This paper is structured as follows: Section 1 introduction explains the research background. Section 2 Mandibular segmentation describes previous research related to mandibular segmentation. Section 3, Enhancement with Ying method, describes Ying research. Section 4 enhancement with DHE method describes DHE research. Section 5 of MobileNetV2 describes MobileNetV2's research. Section 6, Ensemble segmentation, describes segmentation research with ensembles. Section 7 datasets. Section 8 research proposed. Section 9 experimental results enhanced with Ying and DHE methods. Section 10 describes the results of mandibular segmentation and the proposed segmentation ensemble. Section 11 conclusions of the research.

2. Mandibular segmentation

Previous researches have examined mandibular segmentation to achieve good and accurate segmentation performance, as shown in the following Table 1. Previous researches mandibular segmentation were conducted on CT scan images using CNN-based methods, namely SCNN (symmetric convolutional neural network) [2], RCNNSeg [3], U-Net CNN [6]. In addition, researches related to mandibular segmentation in CNN-based CBCT were carried out using the recurrent SegUnet [8], and SASeg [9] methods. The results of mandibular segmentation in previous researches had shortcomings, namely not showing the condyle and coronoid of the mandible clearly. We, therefore, segmented the mandible on a CNN-based panoramic radiograph with MobileNetV2 to display the mandible completely, clearly, and intact.

Table 1. State-of-the-art of the mandibular segmentation

Model name	Research object image dataset	Segmentation results	Model evaluation
Symmetric Convolutional Neural Network (SCNN) [2]	CT scan, Multi-slice computed tomography (MSCT) mandible dataset is collected of the West China Hospital of Stomatology	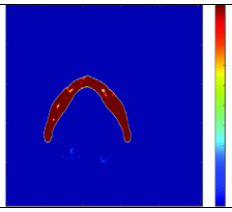	Dice Similarity Coefficient (DSC) 92.02%
RCNNSeg [3]	CT scan, the local University Medical Center Groningen (UMCG), University of Groningen, dataset and the PDDCA public dataset		DSC 95.1 %

Model name	Research object image dataset	Segmentation results	Model evaluation
Fuzzy Connectivity [4]	CT scan, MICCAI 2015 Head-Neck segmentation challenge dataset	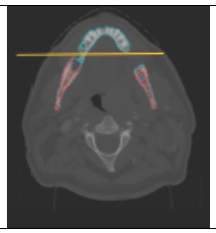	DSC 91%
Conditional statistical shape model [5]	CBCT images collected from dental imaging centers in Tehran and Guilan provinces, Iran	Mandibular Canal 	Average Symmetric Surface Distance (ASSD) ±0.18 and ±0.22
U-Net CNN [6]	CT scan, the collection dataset from the local Medical Ethical Committee	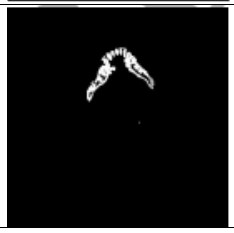	Dice 0.9328
Super-voxels and graph clustering [7]	CBCT, sixteen skull and mandible datasets	Mandibular and skull segmentation 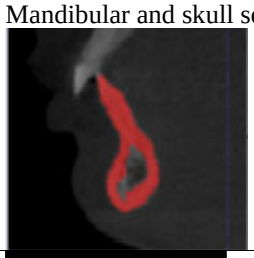	Dice 0.93
Recurrent SegUnet [8]	CBCT dataset, CT dataset from Public Domain Database of the Computational Anatomy (PDDCA) dataset	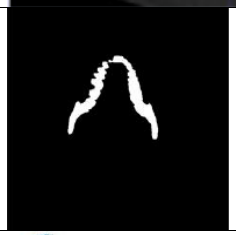	Dice 95.31%
SASeg [9]	CBCT Public Domain Database of the Computational Anatomy (PDDCA) dataset		Dice 95.29%
Active Contour [10]	Panoramic radiography	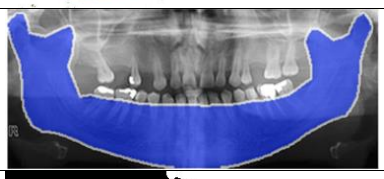	Dice 94.21%
Active Contour+Post Processing [11]	Panoramic radiography	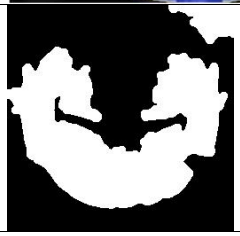	Jaccard Similarity 0.52

Model name	Research object image dataset	Segmentation results	Model evaluation
Transfer Learning CNN (MobileNetV2, ResNet18, ResNet50) [17]	Panoramic radiography		Dice 0.9522

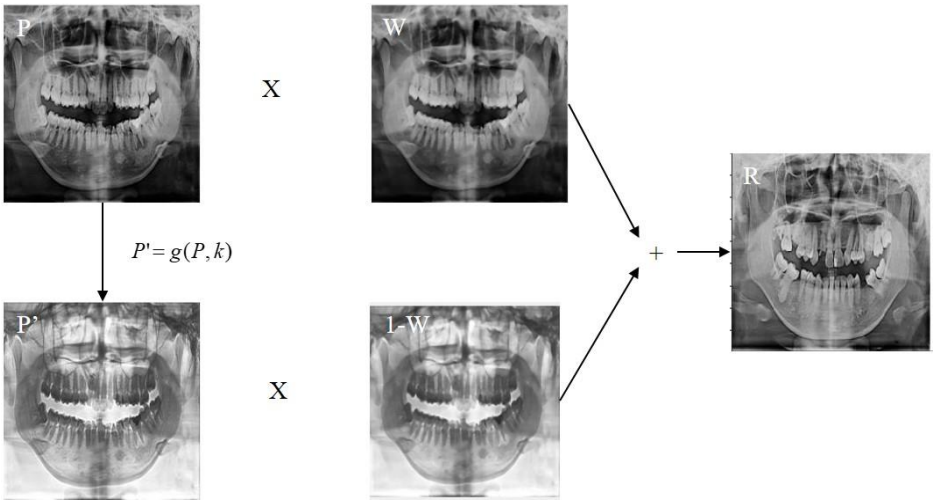

Figure. 1 Enhancement process with Ying method [12, 13]

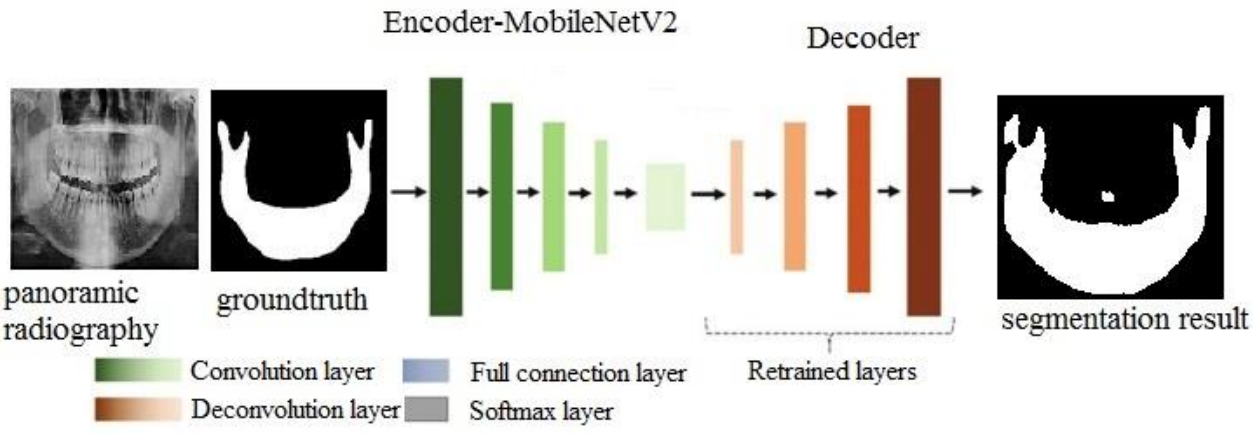

Figure. 2 Segmentation process using MobileNetV2 encoder architecture

3. Enhancement with Ying method

The enhancement of panoramic radiographic images with the Ying algorithm [12, 13] is to make changes based on the intensity and weight values of the image. This enhancement is based on certain areas of the image that have not been exposed in detail. Thus, the image enhanced with the Ying method produces a brighter image. An illustration of the image improvement with Ying is shown in Fig. 1.

4. Enhancement with DHE method

The process of enhancing panoramic radiographic images with the DHE algorithm [14, 15] focuses on spreading high to low intensity values or histogram images, eliminating the dominance of high histograms, and stretching the image intensity values evenly. The DHE method divides the parts of the image and is based on a histogram equalization algorithm. The image divided into several partitions is determined by the

local minimum value of the light intensity. The DHE method makes the initial contrasting image clearer and darker.

5. MobileNetV2

MobileNetV2 deep learning has a small number of parameters, but the performance results are good. MobileNetV2 architecture can be used as an autoencoder for classification, segmentation, or detection. [18] used MobileNetV2 to identify skin cancer with an accuracy of 95.27%. MobileNetV2 is also used for segmentation by implementing an encoder of the MobileNetV2 architecture and adding a decoder architecture [18, 19], as Fig. 2. In [19], the MobileNetV2 method was used as segmentation with a decoder using U-Net architecture, and the performance results were good (IoU 0.7). Based on MobileNetV2's performance in image segmentation in previous researches, we used MobileNetV2 for mandibular segmentation on panoramic radiographs.

6. Ensemble segmentation

Previous researches show that ensemble segmentation for the image using a voting basis had good and optimal performance in processing time and segmentation precision results [16]. Several previous researches on ensemble segmentation for images are listed in Table 2. Ensemble segmentation has been widely carried out in previous researches on medical images. However, many ensemble segmentation methods use the CNN U-Net architecture [20-28], while those based on an encoder of the MobileNetV2 architecture [18, 19] are still little implemented in mandibular segmentation. Example CNN architectures used for segmentation are semi-supervised CNN [29], fully self-adaptive CNN [30], DNN [31], and semantic segmentation convolutional networks [32, 33].

Table 2. State-of-the-art of the ensemble segmentation

Model name	Research object dataset	Segmentation results	Model evaluation
Ensemble U-Net [20]	Breast MRI that has been corrected with DCE. TCGA-BRCA collection was collected by the TCGA Breast Phenotype Research Group and made available in The Cancer Imaging Archive (TCIA)		Dice 0.79 (ensemble union), 0.728 (ensemble majority voting)
Ensemble U-Net, Dilated U-Net, Fractal U-Net, FC-DenseNet, and Pix2Pix (YTU-WaterNet) [21]	Public Landsat 8 OLI satellite image dataset	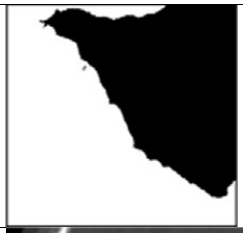	IoU 99.59%
Multi-model ensemble CNN U-Net [22]	Medical image of CT Scan. Dataset of MICCAI 2019 StructSeg challenge	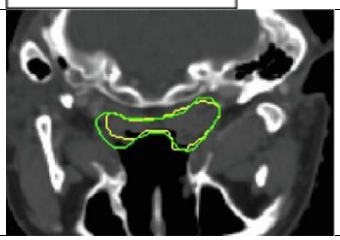	Dice 64.46%
Ensemble U-Net (BUSU-Net) [23]	Medical image, dataset DRIVE		AUC 0.9799
Ensemble CNN U-Net [24]	Medical image of child bone. Public RSNA dataset and clinical CQMU dataset that collected by the Children's Hospital of Chongqing Medical University (CQMU)		Bone age prediction by calculating MAE 5.42

Model name	Research object dataset	Segmentation results	Model evaluation
Ensemble of UNet++, FPN, DeepLabv3, and DeepLabv3+ (DivergentNet) [25]	Medical image, dataset of EndCV2021	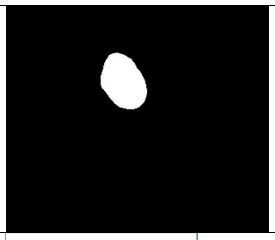	IoU 0.949
Ensemble U-Net [26]	Medical MRI of brain, the WMH Segmentation Challenge at MICCAI 2017		Dice 78.8%
Ensemble U-Net [27]	Citra Colonoscopy, datasets CVC-ColonDB and ETIS-Larib PolypDB from MICCAI 2015 polyp detection challenge	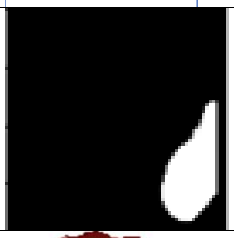	Dice 78.7
Triplanar U-Net ensemble network (TrUE-Net) [28]	MRI image of brain, public dataset (MICCAI WMH Segmentation Challenge 2017, MWSC 2017)	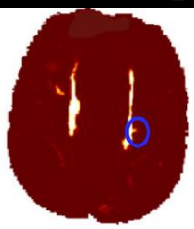	Evaluation metric 0.77
Semi-supervised Deep Convolutional Neural Network [29]	Medical images, ISIC 2018: Skin Lesion Analysis Towards Melanoma Detection grand challenge dataset	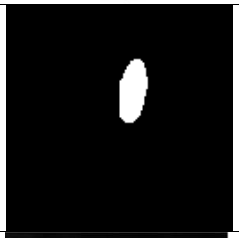	Dice 0.844
Ensemble Fully Convolutional Networks (FCNs) self-adaptive (AdaEn-Net) [30]	Medical MRI, medical image dataset	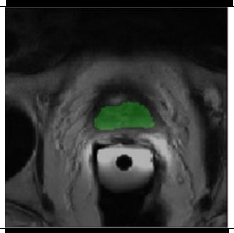	Dice 90.42
Ensemble of DNN [31]	Retinal blood vessels, DRIVE dataset	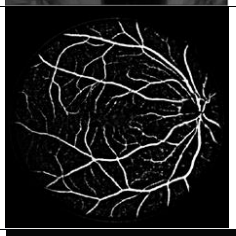	Accuracy 95.33%
Ensemble Semantic Segmentasi Convolutional Networks (ConvNets) [32]	UAV image of vegetation, India Driving Dataset (IDD)	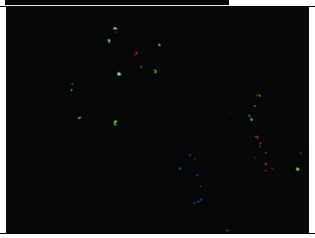	Accuracy 98.14

Model name	Research object dataset	Segmentation results	Model evaluation
Self-assembling of semantic segmentation [33]	MRI image of brain, public MRI dataset	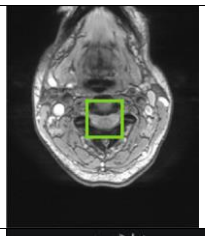	Dice 84.72
Ensemble [34]	Medical image of retina, public DRIVE and STARE dataset		AUC 0.9747
Ensemble Fuzzy C-Means Clustering [35]	Medical image, MR brain image, ISBR database	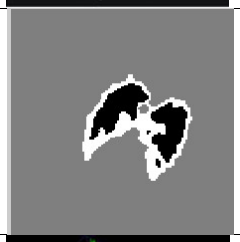	Accuracy 0.7728
Hierarchical view-ensemble convolution (HIVE-Net) [36]	Electron microscopy (EM) image, EPFL dataset, Kasthuri++ dataset	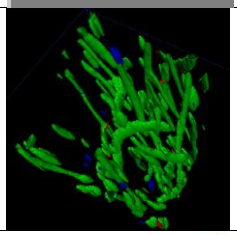	Dice 96.2%
Hypernet ensemble method (HyperNet) [37]	Image, MRI GENIE study		Accuracy 0.891
Multi-Proportion Channel Ensemble Model (MPC-EM) [38]	Medical image of retina, public dataset DRIVE, STARE, HRF and CHASE_DB1	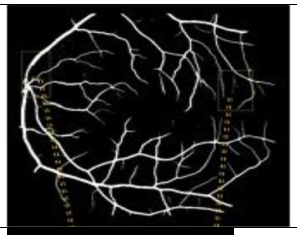	Accuracy 96.54%
Ensemble block matching 3D (BM3D) [39]	Medical image of retina, public dataset Structured Analysis of the Retina (STARE), Digital Retinal Images for Vessel Extraction (DRIVE) and CHASE_DB1	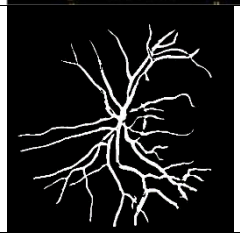	Sensitivity 0.8288
Mojority Vote (diagnose COVID-19) [40]	X-ray iamge, COVID-19 Dataset Award provided by Kaggle Repository		Accuracy 0.993

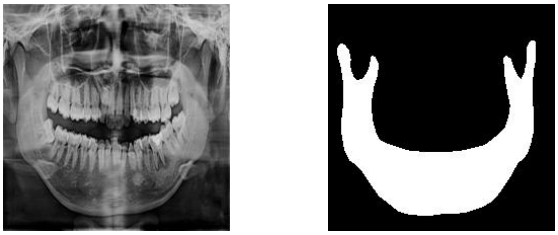

(a) (b)

Figure. 3 (a) Panoramic radiography and (b) Ground truth mandibular

7. Dataset

Panoramic radiography (as in Fig. 3(a)) from the academic dental hospital, Universitas Airlangga, Surabaya, with good quality and has been confirmed by a radiologist. In this research, the sample size used was 38 panoramic radiographs for testing, and 106 panoramic radiographs for modeling. The role of the radiologist is to select a dataset according to the selection criteria. Inclusion criteria: Patient age 19-72 years; Radiographic quality is good, the anatomy of the mandible on the radiograph is clearly visible. Exclusion criteria: Unclear mandibular appearance, e.g., superimposed condylar and coronoid areas with other anatomic features; abnormalities in the mandible, e.g., growth disorders; tumors/cysts; or fracture. In addition, the role of the radiologist is to make ground truth of the mandible on panoramic radiographs. Ground truth (as in Fig. 3(b)) is the mandible's actual data, which has been segmented. The actual data is used as a reference for training the panoramic radiographic data to produce a model. The initial input image is the grayscale image as in Fig. 3(a), the segmentation result as in Fig. 3(b). The input image used in this research is an image size 224 x 224. The sample data has been tested like ethics by the health research ethics eligibility commission (KKEPK) faculty of dentistry, Universitas Airlangga, Surabaya, with certificate number 621/HRECC.FODM/XII/2021.

8. Research proposed

Explanation of Fig. 4 related to the proposed segmentation ensemble is: Original panoramic radiographic data is inputted, and training is carried out with MobileNetV2. The training aims to segment the mandible on a panoramic radiograph. There are panoramic radiographic data that are not good, or too contrasting and too dark so that the enhanced image using the Ying and DHE methods. The original image and the enhanced image using the Ying and DHE methods were trained with MobileNetV2. The three results of MobileNetV2 training are ensemble to produce the best mandibular segmentation. The ensemble method provides very good accuracy in segmentation, and the effectiveness of the ensemble method in neural network segmentation is very good, especially in overcoming the display of missing information.

Figure. 4 The proposed ensemble segmentation method

Deep learning segmentation architectures that are often proposed are encoder and decoder. The encoder changes the input image into a more compact form that summarizes the image information. The decoder is to return spatial information from a summarized. The encoder is the process of compressing the image taking the most important features. At the same time, the decoder is the process of returning complete information. The original image has a size of m x n. The encoder will produce a feature image or image that has been compressed with important information. Then, the decoder will produce the original image size of m x n by returning the information as it was originally. Encoder and decoder are used to segment the mandible on radiographs panoramic. The stages of the mandibular segmentation process using the MobileNetV2 encoder and decoder are shown in Fig. 2. The mandibular segmentation with the proposed ensemble is shown in Fig. 4. Ying and DHE preprocessed the original panoramic radiograph. The enhanced image becomes input in MobileNetV2 training. The image quality enhancement technique proposed by Ying is based on the value of the image's light intensity, which is not conducive. The Ying method produces a good image and reduces contrast, and makes the image brighter. The proposed segmentation ensemble process combines the segmentation results of the original MobileNetV2 image and the enhancement image with based majority voting [16].

9. Experimental results enhance with Ying and DHE methods

The illustration of image enhancement with Ying is shown in Fig. 1. The input image is calculated by calculating the intensity value of each pixel and multiplied by the weight. Calculating the weight of each pixel is based on the image contrast and luminance values. Ying's enhanced image is more dominant in making the image brighter. The enhanced image results with Ying are as shown in Table 3. Table 3 shows that the original image numbers 1, 2 look darker, and the enhanced image using the Ying results are lighter. Table 3 in the original images numbers 2, 3 is bright, and Ying's results also look bright.

The enhanced image process using the DHE method uses the basic histogram equalization formula. The image is divided into several sub-histograms or sections for contrast stretching. The purpose of enhancing the image with DHE is to flatten each image intensity value with a high histogram to a low one. The result image enhancement with DHE makes the image clearer and sharper. The results of image enhancement with DHE are shown in Table 3.

10. Experimental results mandible segmentation and ensemble segmentation

The ensemble segmentation of this research combined the results of mandibular segmentation on panoramic radiographs with MobileNetV2 method. The ensemble segmentation process in this research combines the results of the original image segmentation with the enhanced image using the Ying and DHE methods.

Segmentation ensemble combines the results of many segmentations. The merging process uses the process of adding the value of each pixel from the segmented image. The results of the segmentation and ensemble segmentation processes are shown in Table 4.

As in Table 3, the panoramic radiograph looks very contrast or too bright. Thus, the enhancement is based on the image histogram with the DHE and Ying methods. It aims to enhance the image so that the results of mandibular segmentation are visible complete, and intact. So that when the segmentation results from the original image with the enhanced image using the Ying and DHE methods (Table 3) are combined, the mandible is seen to be more perfect. The process of merging the results of this segmentation is called ensemble segmentation. The purpose is to perform ensemble segmentation to produce a complete, clear, and intact perfect mandible on a panoramic radiograph like the ground truth in Fig. 3(b). Table 4 combines the original image segmentation with the enhanced image using the Ying and DHE methods that are close to the ground truth results (Fig. 3(b)), which means that the ensemble segmentation of Table 4 is successful.

The analysis results of ensemble segmentation show that the original image with image enhancement using the Ying and DHE methods has a higher dice value than MobileNetV2 segmentation results. The results of the dice values from the original image segmentation of the enhanced image using the Ying and DHE methods are shown in Table 5. The proposed segmentation ensemble dice values are shown in Table 5. Based on the average value of the MobileNetV2 segmentation dice in both the original image and the Ying repaired image and DHE the result is too little difference. However, in terms of segmentation results, the combination of the original image with the image enhancement using the Ying and DHE methods provides good segmentation. This is because it can represent the

mandible perfectly, complete, and intact, meaning that the ramus (Condyle, Coronoid), gonial angle, and body of mandible appear all. Overall, the experiment shows that combining the MobileNetV2 segmentation results from the original image selection with the enhanced image using the Ying and DHE methods can produce better segmentation of the mandible because it displays the mandible complete and intact.

One of the evaluation calculations from the segmentation results is calculating the dice value. Eq. (1) is a way to determine the dice value from the segmentation results.

$$dice = \frac{2|A \cap B|}{|A| + |B|} \quad (1)$$

Explanation of Eq. (1), A is the ground truth image, and B is the segmented image.

This research performs segmentation of the mandible on a panoramic radiograph to produce a complete and intact mandible. Mandibular sections on panoramic radiographs can be used for gender identification and age estimation. So we experimented with mandibular segmentation using the MobileNetV2 method because some previous research of segmentation results with MobileNetV2 had a good accuracy of 95.27% [18].

Table 3. Results of enhanced images using Ying and DHE

No	Original image	Image enhancement with Ying	Image enhancement with DHE
1			
2			
3			
4			
5			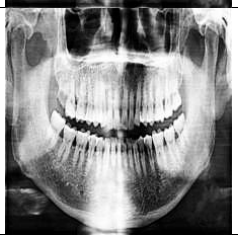

Table 4. Result of image segmentation mandible

No	Original image segmentation results	Enhancement Ying image segmentation results	Enhancement DHE image segmentation results	Ensemble segmentation
1				
2				
3				
4				
5				

Table 5. Average of dice value of ensemble segmentation

Image	Dice average
Original	0.851
DHE	0.855
Ying	0.869
Proposed Ensemble segmentation (Original + Ying + DHE)	**0.9655**

The experimental results of mandibular segmentation on panoramic radiographs using the U-Net and MobileNetV2 methods are shown in Fig. 5. The reason we used MobileNetV2 is that it has a small number of parameters but produces a high dice value compared to U-Net. The results of mandibular segmentation with the U-Net model often do not show the Condyle and Coronoid areas in detail, as shown in Fig. 5(a). Besides the reason for the higher dice value when using the MobileNetV2 model, another reason is that the mandibular segmentation results with MobileNetV2 look more complete (Fig. 5(b)).

Table 6 shows a comparison of previous researches related to mandibular segmentation on panoramic radiography with the researchers' suggestions, with the evaluation results in the research [10] 94.21%, [11] 0.52, [17] 0.9522. The results of the evaluation in Table 6, which are the most superior, are the researchers' suggestions.

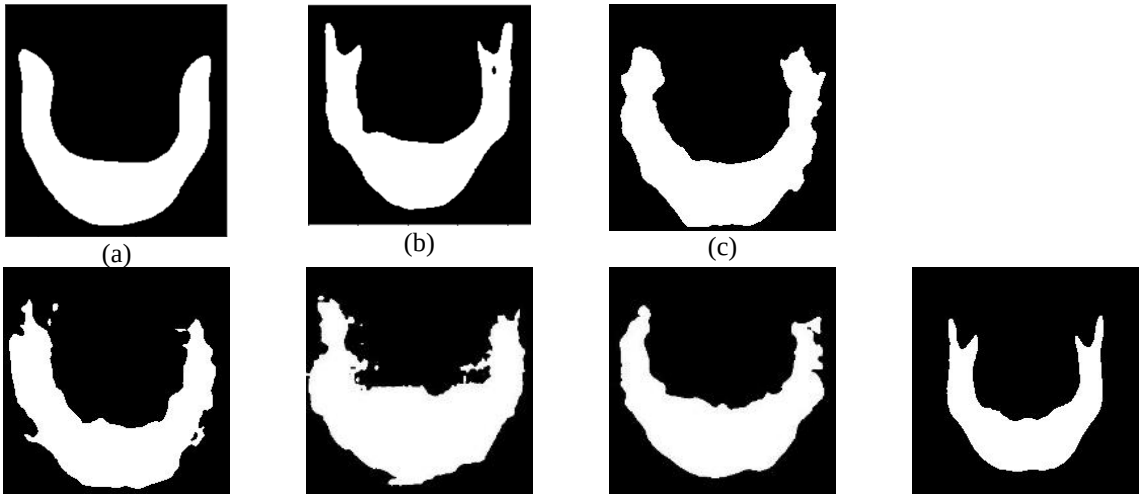

Figure. 5 Segmentation results: (a) U-Net, (b) MobileNetV2, (c) ResNet50, (d) ResNet18, (e) Xception, (f) InceptionResNet V2, and (g) Ensemble MobileNetV2

Table 6. Average evaluation values

Method	Average
Active Contour [10]	94.21%
Active Contour [11]	0.52
MobileNetV2 [17]	0.9522
Ensemble MobileNetV2	**0.9655**

The analysis from Table 4 shows that in the original segmented image, the enhanced image using the Ying and DHE methods have lost information on the coronoid as in image number 2 so that an ensemble can produce a complete mandible. In Table 4, image number 5 results from the original image segmentation ensemble and the enhanced image using the Ying and DHE methods are good, as can be seen in the complete mandibular body. Merging can eliminate black or holes in the middle. In Table 4 number 2, the part of the condyle which was initially lost after the ensemble segmentation was performed can appear complete. The original, Ying, and DHE segmented images cannot represent a perfect mandible (Table 4 number 3). Table 4 images of Ying and DHE segmentation also mostly omit condyle and coronoid information so that the final segmented ensemble can represent the mandible well. The analysis of the segmentation ensemble experiment results is good because it can represent the mandible completely, perfectly, intact, and clearly.

11. Conclusion

The mandibular segmentation process was successfully carried out on panoramic radiographs with the ensemble segmentation method. The image used is a panoramic radiograph. The segmentation ensemble uses the MobileNetV2 encoder and CNN decoder, combining the original image with the enhanced image using the Ying and DHE methods, with a dice value of 0.9655. The results of segmentation of the original image ensemble with a combination of enhanced images using the Ying and DHE methods have a complete and intact mandibular appearance. In the future, we plan to further improve the performance of our model ensemble methods by use transfer learning CNN other.

Conflicts of interest

The authors declare no conflict of interest.

Author contributions

Conceptualization: Nur Nafiiyah, Chastine Fatichah; methodology: Nur Nafiiyah, Chastine Fatichah; software, Nur Nafiiyah; validation, Chastine Fatichah, Darlis Herumurti, Eha Renwi Astuti, and Ramadhan Hardani Putra; resources data, Eha Renwi Astuti, Ramadhan Hardani Putra; writing—original draft preparation: Nur Nafiiyah; writing—review and editing: Nur Nafiiyah, Chastine Fatichah, Darlis Herumurti, Eha Renwi Astuti, and Ramadhan Hardani Putra.

Acknowledgments

Thanks to Deputy for Strengthening Research and Development, Ministry of Research and Technology/National Research and Innovation Agency, Indonesia, for providing research funding

through the Doctoral Dissertation Research scheme with research contract number 1255/PKS/ITS/2020. Thanks to the Dental and Oral Hospital of Universitas Airlangga, Surabaya providing dental radiographic panoramic data.

References

[1] E. R. Astuti, H. B. Iskandar, H. Nasutianto, B. Pramatika, D. Saputra, and R. H. Putra, "Radiomorphometric of the Jaw for Gender Prediction: A Digital Panoramic Study", *Acta Med. Philipp.*, 2021, doi: 10.47895/amp.vi0.3175.

[2] M. Yan, J. Guo, W. Tian, and Z. Yi, "Symmetric convolutional neural network for mandible segmentation", *Knowledge-Based Syst.*, Vol. 159, 2018, doi: 10.1016/j.knosys.2018.06.003.

[3] B. Qiu, J. Guo, J. Kraeima, H. H. Glas, W. Zhang, R. J. H. Borra, M. J. H. Witjes, and P. M. A. V. Ooijen, "Recurrent convolutional neural networks for 3d mandible segmentation in computed tomography", *J. Pers. Med.*, Vol. 11, No. 6, 2021, doi: 10.3390/jpm11060492.

[4] N. Torosdagli, Denise K. Liberton, P. Verma, M. Sincan, J. Lee, S. Pattanaik, U. Bagci, "Robust and fully automated segmentation of mandible from CT scans", In: *Proc. of International Symposium on Biomedical Imaging*, 2017, doi: 10.1109/ISBI.2017.7950734.

[5] F. Abdolali, R. A. Zoroofi, M. Abdolali, F. Yokota, Y. Otake, and Y. Sato, "Automatic segmentation of mandibular canal in cone beam CT images using conditional statistical shape model and fast marching", *Int. J. Comput. Assist. Radiol. Surg.*, Vol. 12, No. 4, pp. 581–593, 2017, doi: 10.1007/s11548-016-1484-2.

[6] B. Qiu, J. Guo, J. Kraeima, H. H. Glas, R. J. H. Borra, M. J. H. Witjes, and P. M. A. V. Ooijen, "Automatic segmentation of the mandible from computed tomography scans for 3D virtual surgical planning using the convolutional neural network", *Phys. Med. Biol.*, Vol. 64, No. 17, 2019, doi: 10.1088/1361-6560/ab2c95.

[7] O. C. Linares, J. Bianchi, D. Raveli, J. B. Neto, and B. Hamann, "Mandible and skull segmentation in cone beam computed tomography using super-voxels and graph clustering", *Vis. Comput.*, Vol. 35, No. 10, 2019, doi: 10.1007/s00371-018-1511-0.

[8] B. Qiu, H. V. D. Wel, J. Kraeima, H. H. Glas, J. Guo, R. J. H. Borra, M. J. H. Witjes, and P. M. A. V. Ooijen, "Mandible Segmentation of Dental CBCT Scans Affected by Metal Artifacts Using Coarse-to-Fine Learning Model", *J. Pers. Med.*, Vol. 11, No. 6, 2021, doi: 10.3390/jpm11060560.

[9] B. Qiu, H. V. D. Wel, J. Kraeima, H. H. Glas, J. Guo, R. J. H. Borra, M. J. H. Witjes, and P. M. A. V. Ooijen, "Robust and accurate mandible segmentation on dental CBCT scans affected by metal artifacts using a prior shape model", *J. Pers. Med.*, Vol. 11, No. 5, 2021, doi: 10.3390/jpm11050364.

[10] A. H. Abdi, S. Kasaei, and M. Mehdizadeh, "Automatic segmentation of mandible in panoramic x-ray", *J. Med. Imaging*, 2015, doi: 10.1117/1.jmi.2.4.044003.

[11] N. Nafi'iyah, C. Fatichah, D. Herumurti, and E. R. Astuti, "The Use of Pre and Post Processing to Enhance Mandible Segmentation using Active Contours on Dental Panoramic Radiography Images", In: *Proc. of 2020 3rd International Seminar on Research of Information Technology and Intelligent Systems*, 2020, doi: 10.1109/ISRITI51436.2020.9315438.

[12] Z. Ying, G. Li, Y. Ren, R. Wang, and W. Wang, "A new image contrast enhancement algorithm using exposure fusion framework", in *Lecture Notes in Computer Science (Including Subseries Lecture Notes In Artificial Intelligence and Lecture Notes In Bioinformatics)*, 2017, Vol. 10425, LNCS, doi: 10.1007/978-3-319-64698-5_4.

[13] Z. Ying, G. Li, Y. Ren, R. Wang, and W. Wang, "A New Low-Light Image Enhancement Algorithm Using Camera Response Model", In: *Proc of 2017 IEEE International Conference on Computer Vision Workshops, ICCVW 2017*, 2017, Vol. 2018-January, doi: 10.1109/ICCVW.2017.356.

[14] M. A. A. Wadud, M. H. Kabir, M. A. A. Dewan, and O. Chae, "A dynamic histogram equalization for image contrast enhancement", *IEEE Trans. Consum. Electron.*, Vol. 53, No. 2, 2007, doi: 10.1109/TCE.2007.381734.

[15] B. S. Rao, "Dynamic Histogram Equalization for contrast enhancement for digital images", *Appl. Soft Comput. J.*, Vol. 89, 2020, doi: 10.1016/j.asoc.2020.106114.

[16] A. Daskalakis, D. Glotsos, S. Kostopoulos, D. Cavouras, and G. Nikiforidis, "A comparative study of individual and ensemble majority vote cDNA microarray image segmentation schemes, originating from a spot-adjustable based restoration framework", *Comput. Methods Programs Biomed.*, Vol. 95, No. 1, pp. 72–88, 2009, doi: 10.1016/j.cmpb.2009.01.007.

[17] N. Nafiiyah, C. Fatichah, D. Herumurti, E. R. Astuti, R. H. Putra, and E. Prakasa, "Mandibular segmentation on panoramic radiographs with CNN Transfer Learning", In: *Proc. of IEEE International Conference on Communication, Networks and Satellite (COMNETSAT)*, pp. 1–5, 2022.

[18] M. Toğaçar, Z. Cömert, and B. Ergen, "Intelligent skin cancer detection applying autoencoder, MobileNetV2 and spiking neural networks", *Chaos, Solitons and Fractals*, Vol. 144, 2021, doi: 10.1016/j.chaos.2021.110714.

[19] J. Jing, Z. Wang, M. Rätsch, and H. Zhang, "Mobile-Unet: An efficient convolutional neural network for fabric defect detection", *Text. Res. J.*, Vol. 92, No. 1–2, pp. 30–42, 2022, doi: 10.1177/0040517520928604.

[20] R. Khaled, J. Vidal, J. C. Vilanova, and R. Martí, "A U-Net Ensemble for breast lesion segmentation in DCE MRI", *Comput. Biol. Med.*, Vol. 140, No. July 2021, p. 105093, 2022, doi: 10.1016/j.compbiomed.2021.105093.

[21] F. Erdem, B. Bayram, T. Bakirman, O. C. Bayrak, and B. Akpinar, "An ensemble deep learning based shoreline segmentation approach (WaterNet) from Landsat 8 OLI images", *Adv. Sp. Res.*, Vol. 67, No. 3, 2021, doi: 10.1016/j.asr.2020.10.043.

[22] H. Mei, W. Lei, R. Gu, S. Ye, Z. Sun, S. Zhang, and G. Wang, "Automatic segmentation of gross target volume of nasopharynx cancer using ensemble of multiscale deep neural networks with spatial attention", *Neurocomputing*, Vol. 438, pp. 211–222, 2021, doi: 10.1016/j.neucom.2020.06.146.

[23] W. H. Khoong, "BUSU-Net: An Ensemble U-Net Framework for Medical Image Segmentation", No. March, 2020, [Online]. Available: http://arxiv.org/abs/2003.01581.

[24] R. Liu, H. Zhu, L. Wang, B. Han, J. Du, and Y. Jia, "Coarse-to-fine segmentation and ensemble convolutional neural networks for automated pediatric bone age assessment", *Biomed. Signal Process. Control*, Vol. 75, No. January, p. 103532, 2022, doi: 10.1016/j.bspc.2022.103532.

[25] V. Thambawita, S. A. Hicks, P. Halvorsen, and M. A. Riegler, "DivergentNets: Medical image segmentation by network ensemble", *CEUR Workshop Proc.*, Vol. 2886, pp. 27–38, 2021.

[26] H. Li, G. Jiang, J. Zhang, R. Wang, Z. Wang, W. S. Zheng, and B. Menze, "Fully convolutional network ensembles for white matter hyperintensities segmentation in MR images", *Neuroimage*, Vol. 183, 2018, doi: 10.1016/j.neuroimage.2018.07.005.

[27] L. T. Thu Hong, N. C. Thanh, and T. Q. Long, "Polyp Segmentation in Colonoscopy Images Using Ensembles of U-Nets with EfficientNet and Asymmetric Similarity Loss Function", In: *Proc. of 2020 RIVF Int. Conf. Comput. Commun. Technol. RIVF 2020*, 2020, doi: 10.1109/RIVF48685.2020.9140793.

[28] V. Sundaresan, G. Zamboni, P. M. Rothwell, M. Jenkinson, and L. Griffanti, "Triplanar ensemble U-Net model for white matter hyperintensities segmentation on MR images", *Med. Image Anal.*, Vol. 73, p. 102184, 2021, doi: 10.1016/j.media.2021.102184.

[29] R. Li, C. Wagner, X. Chen, and D. Auer, "A Generic Ensemble Based Deep Convolutional Neural Network for Semi-Supervised Medical Image Segmentation", In: *Proc. of Int. Symp. Biomed. Imaging*, Vol. 2020-April, pp. 1168–1172, 2020, doi: 10.1109/ISBI45749.2020.9098568.

[30] M. B. Calisto and S. K. L. Yuen, "AdaEn-Net: An ensemble of adaptive 2D–3D Fully Convolutional Networks for medical image segmentation", *Neural Networks*, Vol. 126, pp. 76–94, 2020, doi: 10.1016/j.neunet.2020.03.007.

[31] A. Lahiri, A. G. Roy, D. Sheet, and P. K. Biswas, "Deep neural ensemble for retinal vessel segmentation in fundus images towards achieving label-free angiography", In: *Proc of The Annual International Conference of The IEEE Engineering In Medicine And Biology Society, EMBS*, 2016, Vol. 2016-October, doi: 10.1109/EMBC.2016.7590955.

[32] B. Baheti, S. Innani, S. Gajre, and S. Talbar, "Semantic scene segmentation in unstructured environment with modified DeepLabV3+", *Pattern Recognit. Lett.*, Vol. 138, 2020, doi: 10.1016/j.patrec.2020.07.029.

[33] C. S. Perone, P. Ballester, R. C. Barros, and J. C. Adad, "Unsupervised domain adaptation for medical imaging segmentation with self-ensembling", *Neuroimage*, Vol. 194, No. March, pp. 1–11, 2019, doi: 10.1016/j.neuroimage.2019.03.026.

[34] M. M. Fraz, P. Remagnino, A. Hoppe, B. Uyyanonvara, A. R. Rudnicka, C. G. Owen, and S. A. Barman, "An ensemble classification-based approach applied to retinal blood vessel segmentation", *IEEE Trans. Biomed. Eng.*, Vol. 59, No. 9, 2012, doi: 10.1109/TBME.2012.2205687.

[35] J. Zou, L. Chen, and C. L. P. Chen, "Ensemble fuzzy C-means clustering algorithms based on KL-Divergence for medical image

segmentation", In: *Proc. of 2013 IEEE Int. Conf. Bioinforma. Biomed. IEEE BIBM 2013*, pp. 291–296, 2013, doi: 10.1109/BIBM.2013.6732505.

[36] Z. Yuan, X. Ma, J. Yi, Z. Luo, and J. Peng, "HIVE-Net: Centerline-aware hierarchical view-ensemble convolutional network for mitochondria segmentation in EM images", *Comput. Methods Programs Biomed.*, Vol. 200, p. 105925, 2021, doi: 10.1016/j.cmpb.2020.105925.

[37] S. Hong, A. K. Bonkhoff, A. Hoopes, M. Bretzner, M. D. Schirmer, A. K. Giese, A. V. Dalca, P. Golland, and N. S. Rost, "Hypernet-Ensemble Learning of Segmentation Probability for Medical Image Segmentation with Ambiguous Labels", *arXiv*, 2021, doi: 10.48550/arXiv.2112.06693.

[38] P. Tang, Q. Liang, X. Yan, D. Zhang, G. Coppola, and W. Sun, "Multi-proportion channel ensemble model for retinal vessel segmentation", *Comput. Biol. Med.*, Vol. 111, No. May, p. 103352, 2019, doi: 10.1016/j.compbiomed.2019.103352.

[39] K. Naveed, F. Abdullah, H. A. Madni, M. A. U. Khan, T. M. Khan, and S. S. Naqvi, "Towards automated eye diagnosis: An improved retinal vessel segmentation framework using ensemble block matching 3d filter", *Diagnostics*, Vol. 11, No. 1, pp. 1–27, 2021, doi: 10.3390/diagnostics11010114.

[40] I. Fibriani, Widjonarko, A. Prasetyo, A. M. Raharjo, and D. E. Irawan, "Multi Deep Learning to Diagnose COVID-19 in Lung X-Ray Images with Majority Vote Technique", *Int. J. Intell. Eng. Syst.*, Vol. 13, No. 6, 2020, doi: 10.22266/ijies2020.1231.49.